

# Nucleophilic Fluorination with KF Catalyzed by 18-Crown-6 and Bulky Diols: A Theoretical and Experimental Study

Samuel L. Silva, Marcelo S. Valle, and Josefredo R. Pliego, Jr.\*

Cite This: <https://dx.doi.org/10.1021/acs.joc.0c02229>

Read Online

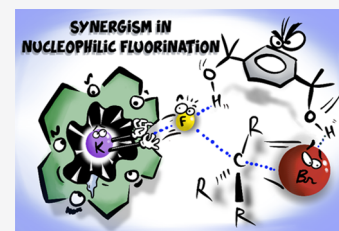
ACCESS |

Metrics & More

Article Recommendations

Supporting Information

**ABSTRACT:** The activation of potassium fluoride for nucleophilic fluorination of alkyl halides is an important challenge because of the high lattice energy of this salt and its low solubility in many polar aprotic solvents. Crown ethers have been used for increasing the solubilization of KF during several decades. Nevertheless, these macrocycles are not enough to produce a high reaction rate. In this work, theoretical methods were used for designing a synergic combination of bulky diols with crown ethers able to accelerate this kind of reaction. The calculations have predicted that the bulky diol 1,4-Bis(2-hydroxy-2-propyl)benzene, which has distant hydroxyl groups, is able to catalyze nucleophilic fluorination in combination with 18-crown-6 via two hydrogen bonds to the  $S_N2$  transition state. Experimental studies following the theoretical predictions have confirmed the catalytic effect and the estimated kinetic data point out that the bulky diol at 1 mol L<sup>-1</sup> in combination with 18-crown-6 is able to produce an 18-fold increase in the reaction rate in relation to crown ether catalysis only. The reaction produces 46% yield of fluorination after 24 h at moderate temperature of 82 °C, with minimal formation of the side elimination product. Thus, this work presents an improved method for fluorination with KF salt.



## INTRODUCTION

Fluorination of aliphatic compounds using fluoride salts as a fluorine source has had an important advance in the past 15 years.<sup>1,2</sup> The discovered bulky alcohols as *tert*-butanol that are more efficient than polar aprotic solvents such as acetonitrile and dimethylformamide for promoting fluorination with CsF salt have shown that both interactions of the solvent with cations and anions are important for accelerating the reaction.<sup>3–5</sup> This different view from the classical paradigm that less anion solvation that leads to a higher reaction rate<sup>6</sup> is due to an important aspect of this reaction: the MF salt has low solubility. Thus, the solvent must have an enough high interaction with the MF salt to overcome the lattice energy in the ionic solid.<sup>7</sup> At the same time, this interaction cannot be so strong to impede the reaction to take place. This important role of both interactions with cations and anions involving CsF salt in *tert*-butanol solvent has also been studied by molecular dynamics methods, which supports the mechanism of an ion pair reaction.<sup>7</sup>

The perception that molecules such as crown ethers, which are able to make strong interaction with the cation,<sup>8,9</sup> could become more effective for solubilizing and activating MF salts due to inclusion of groups able to interact with anions has led to the design of new catalysts.<sup>10</sup> Thus, polyethylene glycols have been investigated and the pentaethylene glycol (Figure 1) was found to be the most effective among them.<sup>11,12</sup> New structures combining calixarene, crown ether, and bulky alcohols (BACCA, Figure 1) were designed and experimentally tested.<sup>13–15</sup> Hydroxylated crown ethers, named hydro-crowns,<sup>16</sup> were also designed, and computational methods have predicted that the additional hydroxyl groups enhance the

catalysis. More recently, theoretical calculations have shown that a new crown ether modified with addition of thiourea groups (thiourea-crown-ether) is very effective for solubilizing and activating KF, even overcoming the [2.2.2]-cryptand.<sup>17</sup>

An important concept in the designing of more effective supramolecular catalysts for nucleophilic fluorination is the idea that the hydrogen bonds should involve the incoming and leaving groups in the  $S_N2$  transition state.<sup>18,19</sup> This effect that was predicted early by theoretical calculations and an envisioned molecule, 1,4-benzenedimethanol (BDM, Figure 1), would have hydroxyl groups in adequate positions for promoting the catalysis.<sup>19</sup> However, due to the formation of aggregates in the solution phase, this effect could be difficult to observe with 1,4-benzenedimethanol.<sup>18</sup> For another structures able to avoid dimerization, such as the BACCA (Figure 1), such an effect is important for explaining quantitatively the observed catalysis.<sup>13,15,20</sup>

Although theory and experiments have shown that the combined functionalities in a single molecule with cation and anion interaction leads to superior catalysis, these newly designed structures involve more molecular complexity.<sup>10</sup> An alternative to this approach is to make the groups with cation and anion interaction to be present in different molecules,

Received: September 15, 2020

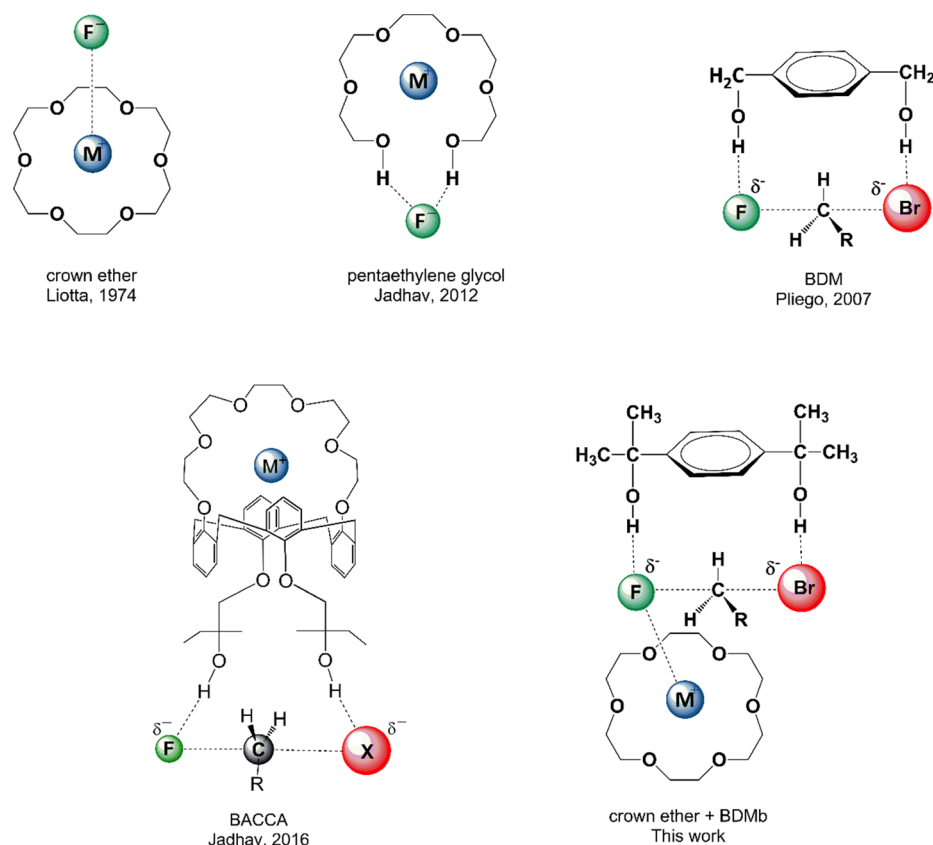
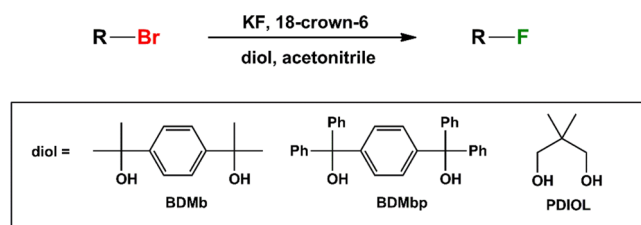


**Figure 1.** Evolution of structures able to interact with cations and/or anions to accelerate  $S_N2$  nucleophilic fluorination.

which would involve simpler structures. Thus, we have hypothesized that the crown ether combined with a diol, 1,4-benzenedimethanol (BDM, Figure 1), could also have a catalytic effect in the fluorination with KF. However, preliminary calculations have indicated that KF-18C6-BDM complex can form a very stable dimer, which could inhibit the catalysis. In order to make this dimer less stable, the hydrogens in the carbons of the  $CH_2OH$  groups were substituted by methyl groups, leading to the bulky diol 1,4-bis(2-hydroxy-2-propyl)benzene, which is named BDMb in this work. The proposed activation mode is presented in Figure 1. In our view, the  $S_N2$  transition state interacts with the bulk diol (BDMb structure) and the fluoride ion remains in close contact with the cation, which is complexed with the crown ether. Such interaction should produce an important rate acceleration effect.

In a previous work, we have investigated the bulky monoalcohol (*tert*-butanol) making hydrogen bonding with the fluoride ion in the KF(18-crown-6) complex and a catalytic effect was theoretically predicted and experimentally observed.<sup>21</sup> In this work, our aim is to analyze if the double hydrogen bonding as envisioned in Figure 1 could be even more effective. Thus, we have performed a detailed theoretical calculation of the model reaction of potassium fluoride with ethyl bromide catalyzed by crown ether combined with the bulky diol BDMb. Further, to evaluate the important role of the position of the hydroxyl groups to promote the catalysis, another diol with close hydroxyl groups, 2,2-dimethyl-1,3-propanediol or neopentyl glycol (named PDIOL), was also investigated. To confirm the theoretical predictions, some selected experiments were also carried out. The reaction is summarized in Scheme 1.

### Scheme 1. Reaction Investigated in This Work



The role of hydrogen bonds involving the fluoride ion is not limited to accelerate the  $S_N2$  reaction. Early experiments by Landini and co-workers involving  $F^-(H_2O)_n$  clusters and tetrabutylammonium as counter ion in apolar solvent showed that more hydrogen bonds lead to more selectivity of the  $S_N2$  reaction versus  $E2$ .<sup>22,23</sup> Theoretical calculations involving catalysis of fluorination by diol<sup>18,19</sup> and tetraol<sup>24</sup> have predicted this trend. Kim et al. have also reported that *tert*-amyl alcohol promotes selective fluorination of alkyl halides with tetrabutylammonium fluoride.<sup>25</sup> More recently, Gouverneur and co-workers reported a detailed investigation of the effect of stoichiometric diverse bulky alcohols<sup>26</sup> and ureas<sup>27</sup> with specific solvation to the fluoride ion in acetonitrile solvent. The same trend of  $S_N2$  selectivity promoted by hydrogen bonding was observed. Thus, the present study also evaluates the selectivity of  $S_N2$  product in the catalysis by 18-crown-6 combined with bulky diols.

## RESULTS AND DISCUSSION

In the phase-transfer-catalyzed fluorination of alkyl halide (or mesylate) with KF salt, it is important to consider two steps:

the solubilization of the salt, formation of the KF(cat) complex, and the activation step involving the KF(cat) complex in the transition state. In order to have insights in the interactions involved, we have first analyzed the formation of the complexes involving KF, crown ether, and the bulky diols BDMb and PDIOL. In the next step, the activation process was analyzed and in the third step, the free energy profile.

The complexes involving KF, 18-crown-6 and bulky diols are presented in Figure 2. In the case of the complex with BDMb,

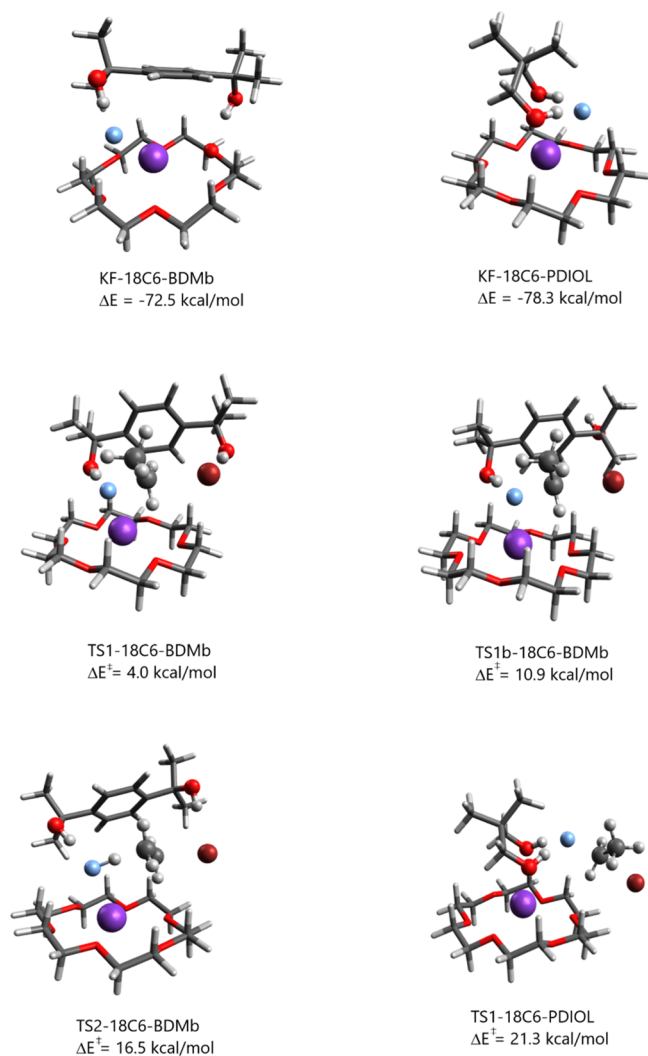


**Figure 2.** Complexes and transition states involving KF, 18-crown-6, and the diols BDMb and PDIOL. The values of  $\Delta E$  correspond to the formation of the complexes from the separated species (KF, 18-crown-6, and the diol). The activation barriers ( $\Delta E^\ddagger$ ) correspond to  $S_N2$  and E2 transition states from the KF-18C6-diol + EtBr taken as reference. Energies from LPNO-CEPA calculations. Atoms: oxygen (red), carbon (gray), fluorine (light blue), bromine (wine), and potassium (purple).

the fluoride ion interacts with both the potassium ion and with one hydroxyl of the BDMb. The second hydroxyl from BDMb also makes a hydrogen bond with one oxygen from 18-crown-6. The structure also suggests some cation- $\pi$  interaction between the  $K^+$  and the aromatic ring from BDMb. The total interaction energy in this complex from KF (gas phase) + 18-crown-6 + BDMb reference state is 72.5 kcal mol<sup>-1</sup>, a very

substantial value. In the case of only KF + 18-crown-6, the interaction energy reported is only 41.7 kcal mol<sup>-1</sup>. Thus, the addition of BDMb diol should be able to produce a substantial increase in the solubilization of KF salt. In the same way, the PDIOL molecule has also high interaction energy with the fluoride ion and the KF-18C6-PDIOL complex is stable by 78.3 kcal mol<sup>-1</sup>, as shown in Figure 2. There are two hydrogen bonds between hydroxyls from PDIOL and the fluoride ion, and the oxygens from PDIOL also interact with the potassium ion. Thus, both complexes are very stable.

The second step is the activation, involving the reaction with ethyl bromide via the  $S_N2$  transition state. It is worth to analyze the intrinsic reactivity, without the solvent effect. In this situation, very high difference can be noted for the complexes. The energy barrier for the KF-18C6-BDMb and EtBr reaction model via TS1-18C6-BDMb is 4.0 kcal mol<sup>-1</sup>, whereas it becomes 21.3 kcal mol<sup>-1</sup> in the case of TS1-18C6-PDIOL. For comparison, the  $\Delta E^\ddagger$  barrier (Table S1, Supporting Information) for the KF-18C6 + EtBr reaction is 3.7 kcal mol<sup>-1</sup>. With the addition of *tert*-butanol as alcohol, the barrier becomes 12.7 kcal mol<sup>-1</sup>.<sup>21</sup> Thus, the energy barrier via the KF-18C6-BDMb complex is as low as the energy barrier for the reaction via the KF-18C6 complex. These differences can be attributed to how the diols interact with the transition state. The BDMb species interact with both the incoming fluoride ion and the leaving bromide ion. Thus, there is an additional hydrogen bonding with a highly charged group (the leaving Br). To provide more support for the role of the second hydroxyl, another  $S_N2$  transition state involving BDMb, named TS1b-18C6-BDMb and without this second hydrogen bond, was located (Figure 2). In this case, the  $\Delta E^\ddagger$  barrier becomes 10.9 kcal mol<sup>-1</sup>, close to the *tert*-butanol barrier. In the case of PDIOL, its strong interaction with the fluoride ion in the KF-18C6-PDIOL complex is substantially decreased in the TS1-18C6-PDIOL structure because part of the charge in the fluoride ion is transferred to the leaving Br. As a consequence, a high barrier is induced. Thus, this simple analysis indicated that the diol with more distant hydroxyls (BDMb) able to interact with the entering and leaving groups should be more effective. Nevertheless, the solvent effect, entropy, and solubility need be taken into account for a reliable prediction on the ability of these alcohols to accelerate the  $S_N2$  reaction. Finally, the E2 mechanism was also investigated and the respective transition state, TS2-18C6-BDMb, has a high  $\Delta E^\ddagger$  barrier of 16.5 kcal mol<sup>-1</sup>. This result indicates an important selectivity induced by the BDMb toward the  $S_N2$  mechanism because the barrier for E2 catalyzed by 18-crown-6 only is 8.1 kcal mol<sup>-1</sup>.<sup>21</sup>

**Formation of Aggregates.** In the theoretical prediction of catalytic processes, it is important to evaluate what species are present in the solution phase. The formation of stable aggregates can produce an increase in the observed free energy barrier and eliminate any possible catalysis. Thus, we have evaluated the formation of aggregates of KF-18C6 with two BDMb molecules and also the possibility of the dimerization of the KF-18C6-BDMb species. In this investigation, the structures presented in Figure 3 were obtained. The KF-18C6-BDMb<sub>2</sub> complex is formed by the addition of one more BDMb molecule to the KF-18C6-BDMb complex. The fluoride ion makes two hydrogen bonds, and there is an additional hydrogen bond between the hydroxyls from BDMb. The addition of the second BDMb molecule has  $\Delta E = -27.7$  kcal mol<sup>-1</sup>. The other aggregate, (KF-18C6-BDMb)<sub>2</sub>, is the

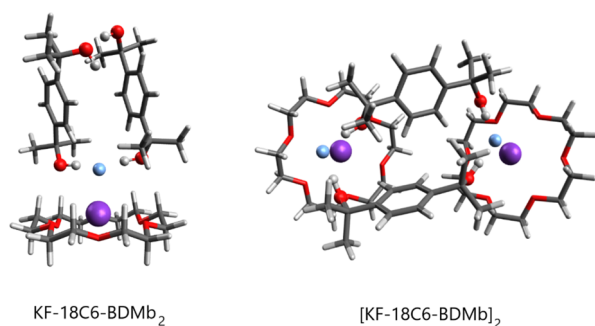


**Figure 3.** Higher aggregates that can be formed involving KF-18C6 and BDMb.

dimerization of the KF-18C6-BDMb complex, and the corresponding  $\Delta E$  for dimerization is  $-38.9 \text{ kcal mol}^{-1}$ . Thus, both aggregates have a strong interaction energy and could be important in inhibition of the catalysis. Thus, these species were considered in the calculation of the free energy profile of the reaction.

**Free Energy Profile.** In order to predict quantitatively any catalytic effect, it is needed to generate the free energy profile for each step, including the solubilization of the KF salt. The catalysis by 18-crown-6 and BDMb is presented in Figure 4. For completeness, the previously reported catalysis by 18-crown-6, studied in the same level of theory, was also included.

The solubilization of the solid KF salt by 18-crown-6 in acetonitrile has a free energy of  $8.8 \text{ kcal mol}^{-1}$ , and considering the activation step, the final  $\Delta G^\ddagger$  barrier is  $32.0 \text{ kcal mol}^{-1}$ . This value is compatible with the experimental kinetics which requires long reaction time and refluxing conditions. With the addition of BDMb to the medium, forming the KF-18C6-BDMb complex, the solubilization increases and the free energy decreases to  $3.8 \text{ kcal mol}^{-1}$ . The activation step involves the TS1-18C6-BDMb transition state with a  $\Delta G^\ddagger$  barrier of  $24.3 \text{ kcal mol}^{-1}$ , a substantial decrease by  $7.7 \text{ kcal mol}^{-1}$  from the crown ether catalysis. Thus, in the absence of another equilibrium able to stabilize the pre-reactive complex, a very meaningful catalytic effect is predicted by the combination of crown ether and BDMb. The formation of aggregates presented in Figure 3 could make the reaction slower or

even eliminate any catalytic effect. Thus, the free energy of these species was also analyzed and included in the free energy profile. The addition of a second molecule of BDMb, forming the KF-18C6-BDMb<sub>2</sub> species leads to higher stability, and the free energy decrease to  $0.9 \text{ kcal mol}^{-1}$ . In the case of the dimerization of the KF-18C6-BDMb, forming the (KF-18C6-BDMb)<sub>2</sub> species, the free energy becomes  $1.7 \text{ kcal mol}^{-1}$ , taking into account the stoichiometry of the process. Thus, based on these results, the formation of these complexes should not decrease the predicted catalysis in acetonitrile. However, in a less polar solvent, these complexes should become more stable and have negative free energy, which could result in inhibition of catalysis. Any theoretical investigation of this kind of catalysis must consider the possible formation of aggregates. Otherwise, reliable predictions cannot be done.

The calculations predict that the E2 transition state (TS2-18C6-BDMb in Figure 2) is much less favorable than the S<sub>N</sub>2 one, with a free energy barrier  $5 \text{ kcal mol}^{-1}$  higher than the S<sub>N</sub>2 pathway (Table S1). Based on this data, only a trace of the E2 product should be formed by this catalysis.

Considering the free energy profile, the rate law is predicted to be given by:

$$\frac{d[\text{RBr}]}{dt} = -k[\text{BDMb}][\text{18C6}][\text{RBr}] \quad (1)$$

with the rate constant  $k$  related to  $\Delta G^\ddagger = 24.3 \text{ kcal mol}^{-1}$ . The derivation is presented in the Supporting Information.

The theoretical free energy profile in Figure 4 shows that the present combination of BDMb with 18-crown-6 leads to a true catalytic system, with release of the diol and of the crown ether. The formed KBr-18C6-BDMb complex (and RF product) has a relative free energy of  $-7.4 \text{ kcal mol}^{-1}$ . The release of the BDMb, forming KBr-18C6, is favorable, and its free energy is  $-8.5 \text{ kcal mol}^{-1}$ . This result shows that BDMb does not form a favorable complex with KBr-18C6. A different behavior occurs for KF-18C6 because complexation with BDMb decreases the free energy from  $8.8$  to  $3.8 \text{ kcal mol}^{-1}$ . Further, the KBr-18C6 complex has relative free energy of  $-8.5 \text{ kcal/mol}$  and when the dissociation of this complex takes place, forming solid KBr and free 18-crown-6, the free energy

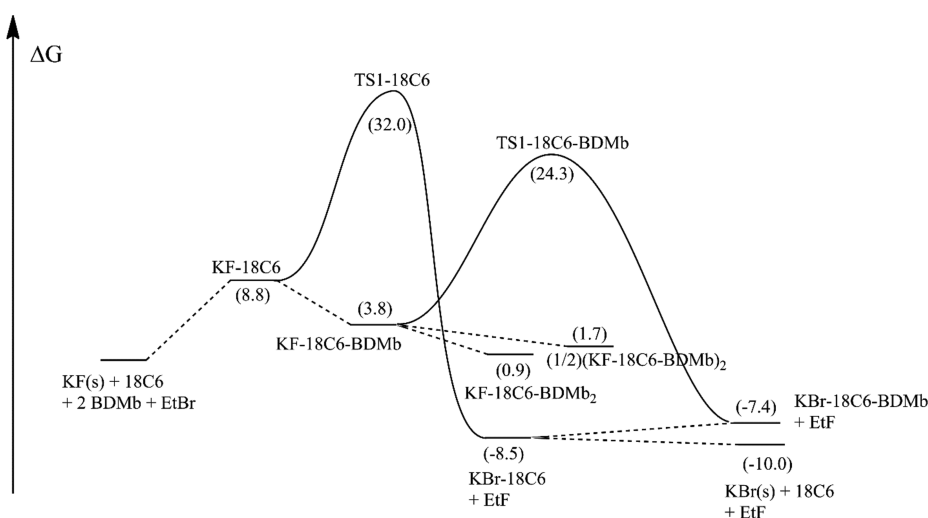


**Figure 4.** Free energy profile for the KF(s) + 18-crown-6 + BDMb reaction in acetonitrile solvent. Calculations at LPNO-CEPA1/ma-def2-TZVPP//PBE/ma-def2-SVP level of theory. Solvent effect calculated by the SMD model.

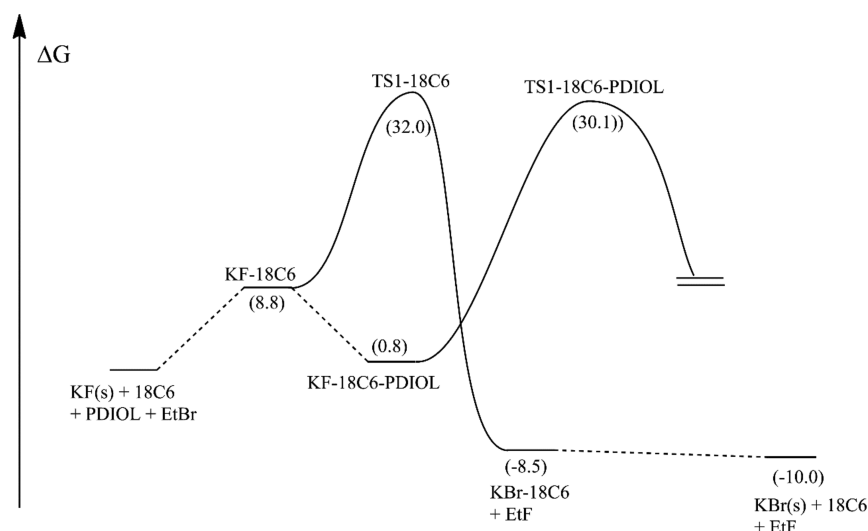
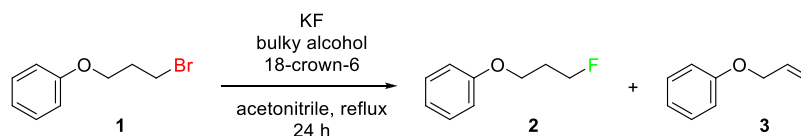


**Figure 5.** Free energy profile for the KF(s) + 18-crown-6 + PDIOL reaction in acetonitrile solvent. Calculations at the LPNO-CEPA1/ma-def2-TZVPP//PBE/ma-def2-SVP level of theory. Solvent effect calculated by the SMD model.

**Table 1. Experiments of Fluorination Reactions<sup>a</sup>**



entry	KF (mmol)	bulky alcohol	bulky alcohol (mmol)	yield (%) of 2	yield (%) of 3	ref
1	2			4.7	trace	21
2	2	<i>tert</i> -butanol	1	13.5	3.5	21
3	2	BDMb	1	22	trace	this work
4	2	BDMb	3	46	3	this work
5	2	BDMbp	1	17	trace	this work

<sup>a</sup>Experiments using 1 mmol of (3-bromopropoxy)benzene, 1 mmol of 18-crown-6, and 4 mL of the acetonitrile solvent. The reaction mixture was heated to reflux (82 °C) during 24 h.

becomes  $-10.0 \text{ kcal mol}^{-1}$ , which is  $1.5 \text{ kcal mol}^{-1}$  below KBr-18C6. Thus, both the 18C6 and BDMb are free for a new catalytic cycle. Therefore, it is a true catalysis. Based on the kinetic law, we could use sub-stoichiometric concentration of both BDMb and 18C6. However, in the experimental part, we have used stoichiometric quantities of the BDMb and 18-crown-6 to produce a faster kinetics. In our view, more design of the diol could lead to a more enhanced rate acceleration effect and more efficient catalysis.

The free energy profile for the reaction catalyzed by another diol (PDIOL) was also calculated and is presented in Figure 5. The strong interaction of this diol with KF-18C6 leads to an even more stable complex, KF-18C6-PDIOL, with a free energy of only  $0.8 \text{ kcal mol}^{-1}$ . However, as expected from previous analysis, the activation step is very unfavorable and the  $\Delta G^\ddagger$  considering the solubilized KF-18C6-PDIOL complex is  $29.3 \text{ kcal mol}^{-1}$ . For comparison, in the case of BDMb, this same barrier is  $20.5 \text{ kcal mol}^{-1}$ . Nevertheless, because the PDIOL leads to better solubilization, the overall  $\Delta G^\ddagger$  considering the solid KF is  $30.1 \text{ kcal mol}^{-1}$ . Thus, the calculation predicts that even this diol has a small catalytic effect and the decrease in the  $\Delta G^\ddagger$  in relation to the 18-crown-6 catalysis is predicted to be  $1.9 \text{ kcal mol}^{-1}$ .

The present theoretical results suggest that diols similar to BDMb, with distant hydroxyls, should be more effective for catalysis than diols with close hydroxyls. On the other hand,

formation of two hydrogen bonds with the fluoride ion makes the solubilization more favorable. Such an observation also suggests that a tetraol with distant pairs of hydroxyls like NPTROL could produce a further enhanced catalytic effect.<sup>24</sup> Another interesting observation is that Gouverneur and co-workers have also reported that the diol neopentyl glycol has produced substantially less reactivity in fluorination with tetrabutylammonium fluoride than bulky monoalcohols, in line with the present report.<sup>26</sup>

## EXPERIMENTAL RESULTS

Based on the theoretical studies, a structure like BDMb should be effective to provide the catalysis, whereas PDIOL should not. Thus, we have investigated experimentally the reaction in Scheme 1 using BDMb and BDMbp as diols. The reaction was carried out in acetonitrile solvent, under reflux (82 °C) and using 2 mmol of KF, 1 mmol of 18-crown-6, and 1 to 3 mmol of the diols. The results are presented in Table 1, and we have included the results of a previous study using *tert*-butanol as bulky alcohol for comparison.<sup>21</sup>

In the reaction catalyzed by 18-crown-6, the fluorination yield is only 4.7% after 24 h (entry 1). With the use of 1 mmol of *tert*-butanol in our previous report (entry 2), the yield increased to 13.5%. In the case of the BDMb diol used in this work, the yield was 22% (entry 3), almost twice the yield with *tert*-butanol using 1 mmol. With the increase of the concentration of BDMb (use of 3 mmol), the yield reached 46%, in line with eq 1 that predicts linear dependence of the kinetics with the concentration of BDMb. In the last experiment

(entry 5), using the BDMbp diol, the yield was smaller than that observed for BDMb. Thus, the present experiments point out that a combination of 18-crown-6 with the BDMb diol produces a substantial increase of the phase-transfer-catalyzed fluorination of a primary alkyl bromide in relation to the use of 18-crown-6 only. Furthermore, the BDMb is more efficient than *tert*-butanol to accelerate the reaction.

Another important aspect of this study is the high selectivity observed for crown ether-BDMb catalysis. In entry 4, the fluorination yield was 46%, while the E2 yield was only 3%. The  $S_N2/E2$  ratio is 15, a substantially better value than that reported for complexes of bulky alcohols with tetrabutylammonium fluoride,<sup>26</sup> which are in the range from 1 to 4.

**Comparison between Theory and Experiment.** The experimental data can be used for estimating  $\Delta G^\ddagger$  and for making a comparison with theoretical values. Thus, we need to consider a kinetic model. Based on the calculation of the free energy profile, we can consider the rate law for alkyl bromide decay as:

$$\frac{d[\text{RBr}]}{dt} = -(k_c + k_{cd}[\text{BDMb}]][18\text{C6}][\text{RBr}] \quad (2)$$

where  $k_c$  is the rate constant for crown ether catalysis and  $k_{cd}$  is the rate constant for crown ether and diol catalysis. Based on the data in Table 1, we have considered the concentration of alkyl bromide and crown ether as 0.25 mol L<sup>-1</sup>, while the diol is 0.25 mol L<sup>-1</sup> (1 mmol) and 0.75 mol L<sup>-1</sup> (3 mmol). The reaction rate for alkyl bromide decay can be rewritten as:

$$\frac{d[\text{RBr}]}{dt} = -k_{\text{eff}}[\text{RBr}] \quad (3)$$

where  $k_{\text{eff}}$  is the pseudo-first order rate constant given by:

$$k_{\text{eff}} = (k_c + k_{cd}[\text{BDMb}]][18\text{C6}] \quad (4)$$

Considering the reaction time and the yield (conversion), we can estimate  $k_{\text{eff}}$  by the first-order decay:

$$[\text{RBr}]_t = [\text{RBr}]_0 \cdot e^{-k_{\text{eff}}t} \quad (5)$$

Thus, the 4.7% conversion in Table 1 (entry 1) leads to  $k_{\text{eff}} = 5.6 \times 10^{-7} \text{ s}^{-1}$  and because  $[18\text{C6}] = 0.25 \text{ mol L}^{-1}$ , we can estimate that  $k_c = 2.2 \times 10^{-6} \text{ mol}^{-1} \text{ s}^{-1}$ . Once the rate constant is known, the  $\Delta G^\ddagger$  can be determined from the transition state theory and the temperature of the reaction. This procedure was applied for entries 1 to 5 in Table 1 to estimate the rate constants and the respective  $\Delta G^\ddagger$ , which are presented in Table 2.

**Table 2. Estimated Experimental Kinetic Parameters Based on a Simple Analysis of the experiments<sup>a</sup>**

entry	$k_{\text{eff}}$ (s <sup>-1</sup> )	$k_c$ (L mol <sup>-1</sup> s <sup>-1</sup> )	$\Delta G^\ddagger$ (kcal mol <sup>-1</sup> )
1	$5.6 \times 10^{-7}$	$2.2 \times 10^{-6}$	30.1 <sup>b</sup>
entry	$k_{\text{eff}}$ (s <sup>-1</sup> )	$k_{cd}$ (L <sup>2</sup> mol <sup>-2</sup> s <sup>-1</sup> )	$\Delta G^\ddagger$ (kcal mol <sup>-1</sup> )
2	$1.7 \times 10^{-6}$	$1.8 \times 10^{-5}$	28.6 <sup>b</sup>
3	$2.9 \times 10^{-6}$	$3.7 \times 10^{-5}$	28.1
4	$7.1 \times 10^{-6}$	$3.5 \times 10^{-5}$	28.2
5	$2.2 \times 10^{-6}$	$2.6 \times 10^{-5}$	28.4

<sup>a</sup>Values determined based on the data from Table 1 and the kinetic equations 2–5. <sup>b</sup>Taken from ref 21.

The free energy barrier for crown ether catalysis was reported in our previous study and the experimental estimate is 30.1 kcal mol<sup>-1</sup>, close to the theoretical value of 32.0 kcal mol<sup>-1</sup>. In the case of the addition of *tert*-butanol, both theory and experiments are also in very good agreement with the theoretical barrier predicted to be 28.4 kcal mol<sup>-1</sup>, whereas the experimental value is 28.6 kcal mol<sup>-1</sup>.<sup>21</sup> It is worth to say that another two experiments with *tert*-butanol led to a slightly lower experimental barrier of 28.3 kcal mol<sup>-1</sup>. However, those experiments have involved more concentrated solutions and longer

reaction time. Thus, we think that a comparison using 0.25 mol L<sup>-1</sup> and a shorter reaction time is more adequate because it avoids aggregation effects and possible secondary reactions that can occur in a longer reaction time.

In the case of crown ether and BDMb catalysis, entry 3 leads to an experimental free energy barrier of 28.1 kcal mol<sup>-1</sup>, whereas higher concentration of BDMb (entry 4) leads to a slightly higher value of 28.2 kcal mol<sup>-1</sup>. The predicted theoretical  $\Delta G^\ddagger$  is 24.3 kcal mol<sup>-1</sup>, a difference of 3.8 kcal mol<sup>-1</sup>. This is a reasonable agreement, although the theoretical accuracy is not so good as that obtained for *tert*-butanol catalysis. Thus, the rate acceleration effect predicted by theory due to addition of BDMb to crown ether catalysis is experimentally verified. However, the observed effect is smaller than predicted by theory. Another bulk diol (BDMbp) was also experimentally tested (entry 5) and the estimated  $\Delta G^\ddagger$  was 28.4 kcal mol<sup>-1</sup>, slightly higher than the BDMb catalysis. This result indicates that there is no advantage of using this more complex molecule.

A question that arises is what is the reason for the error in the theoretical calculations to be higher for the BDMb catalysis than for *tert*-butanol? In part, the error in the theory is due to the temperature used in the calculations (25 °C) while the experiments were done at 82 °C. A substantial  $-T\Delta S$  term is expected because the transition state merges three species to form the transition state. As a rough estimate, considering  $\Delta S = -50 \text{ cal K}^{-1} \text{ mol}^{-1}$ , the variation of the  $-T\Delta S$  term is  $(-T_2\Delta S + T_1\Delta S) = -\Delta T\Delta S$ . When going from 25 to 82 °C,  $\Delta T = 57 \text{ K}$  and we can calculate that  $-\Delta T\Delta S = 2.9 \text{ kcal mol}^{-1}$ , which increases  $\Delta G^\ddagger$  to 27.2 kcal mol<sup>-1</sup> at 82 °C, very close to the experimental value of 28.1 kcal mol<sup>-1</sup>. On the other hand, such an effect would also increase the error in barrier predicted for the *tert*-butanol catalysis (see ref 21). In our opinion, it would be desirable to use more reliable theoretical methods, including explicit solvent molecules and better treatment of low vibrational frequencies to make more accurate predictions. Nevertheless, it is important to say that the present theoretical approach was able to correctly predict the catalytic effect and has guided the experiments toward the proof of this kind of catalysis. Further optimization of experimental conditions and use of another diol structure could lead to more effective catalysis and even stereochemical control via chiral diols.

## CONCLUSIONS

The combined effect of 18-crown-6 and bulky diol (BDMb) for phase-transfer-catalyzed fluorination of an alkyl bromide using potassium fluoride reagent was investigated by theoretical methods and experiments. The calculations indicate the BDMb works by stabilizing the  $S_N2$  transition state via two hydrogen bonds to the incoming and leaving groups. Thus, a catalytic effect was predicted for this combination, which was confirmed by the experiments. Based on the estimated experimental kinetic data, using BDMb at 1 mol L<sup>-1</sup> concentration combined with crown ether leads to rate acceleration by 18-fold in relation to crown ether catalysis only. In addition, the catalyzed reaction is highly selective, producing a minimal E2 product. Therefore, this study presents an improved fluorination method using the KF reagent, 18-crown-6, and the bulky diol BDMb.

## EXPERIMENTAL SECTION

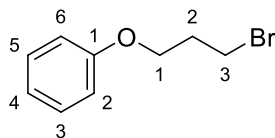
**NMR Analysis.** Proton (<sup>1</sup>H) and carbon (<sup>13</sup>C{<sup>1</sup>H}) NMR spectra were recorded on a Bruker 500 MHz in CDCl<sub>3</sub> spectrometer at the Federal University of Juiz de Fora. Chemical shifts ( $\delta$ ) are reported in parts per million with reference to residual CHCl<sub>3</sub> (<sup>1</sup>H, 7.26; <sup>13</sup>C, 77.00).

**General Procedure.** (3-Bromopropoxy)benzene (1.00 mmol, 158.00  $\mu\text{L}$ , purchased from Sigma-Aldrich) was added to a solution of potassium fluoride (2.00 mmol), 18-crown-6 (1.00 mmol), 1,4-bis(2-hydroxyisopropyl)benzene or 1,4-bis(diphenylhydroxymethyl)-

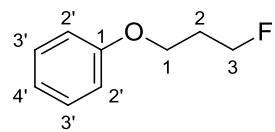
benzene (1.00 or 3.00 mmol) in acetonitrile (directly from the bottle), and the reaction was refluxed in an oil bath for 24 h. The solvent of the reaction was concentrated under reduced pressure, and purification of the resulting residue by flash chromatography on silica gel (EtOAc/heptane 05:95) (to remove essentially the crown ether) afforded a pale yellow oil. In this stage, the oil obtained was analyzed by NMR. The yields were calculated by integration of the spectra of  $^1\text{H}$  NMR and are showed in Table 1.

### Spectroscopy Data.

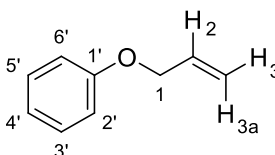
#### Spectroscopy data



(3-Bromopropoxy)benzene. Colorless liquid.  $^1\text{H}$  NMR ( $\text{CDCl}_3$ , 500 MHz):  $\delta$  7.39 (2H, H-3',  $J$  7.3 Hz, t), 7.06 (1H, H-4',  $J$  7.3 Hz, t), 2.39 (2H, H-2,  $J$  6.1 Hz, quint), 7.01 (2H, H-2',  $J$  8.5 Hz, d), 4.17 (2H, H-1,  $J$  6.0 Hz, t), 3.68 (2H, H-3,  $J$  6.4 Hz, t).  $^{13}\text{C}\{^1\text{H}\}$  NMR ( $\text{CDCl}_3$ , 125 MHz):  $\delta$  158.8 (C-1'), 129.6 (C-3'), 121.0 (C-4'), 114.6 (C-2'), 65.3 (C-1), 32.5 (C-3), 30.2 (C-2).



(3-Fluoropropoxy)benzene (Ref 28. Colorless oil.  $^1\text{H}$  NMR ( $\text{CDCl}_3$ , 500 MHz):  $\delta$  7.39 (2H, H-3',  $J$  7.3 Hz, t), 7.06 (H-4', 1H,  $J$  7.3 Hz, t), 7.01 (2H, H-2',  $J$  8.5 Hz, d), 4.65 (2H, H-3,  $J$  47.0 Hz,  $J$  6.0 Hz, dt), 4.10 (2H, H-1,  $J$  6.0 Hz, t), 2.16 (2H, H-2, dq,  $J$  25.9 Hz,  $J$  6.0 Hz, dq).  $^{13}\text{C}\{^1\text{H}\}$  NMR ( $\text{CDCl}_3$ , 125 MHz):  $\delta$  158.8 (C-1'), 129.6 (C-3'), 121.0 (C-4'), 114.6 (C-2'), 80.8 (C-3,  $J$  164.0 Hz, d), 63.5 (C-1), 30.4 (C-2',  $J$  20.0 Hz, d).



(Allyloxy)benzene (Ref 29. Colorless solid.  $^1\text{H}$  NMR ( $\text{CDCl}_3$ , 500 MHz):  $\delta$  7.39 (2H, H-3',  $J$  7.3 Hz, t), 7.06 (1H, H-4',  $J$  7.3 Hz, t), 7.01 (2H, H-2',  $J$  8.5 Hz, d), 6.01 (1H, H-2,  $J$  17.0 Hz,  $J$  10.5 Hz,  $J$  5.3 Hz, dq), 5.47 (1H, H-3a,  $J_{trans}$  17.0 Hz,  $J_{gem}$  1.5 Hz, dd), 5.30 (1H, H-3,  $J_{cis}$  10.5 Hz,  $J_{gem}$  1.5 Hz, dd), 4.57 (2H, H-1,  $J$  5.3 Hz, d).  $^{13}\text{C}\{^1\text{H}\}$  NMR ( $\text{CDCl}_3$ , 125 MHz):  $\delta$  158.8 (C-1'), 133.5 (C-2), 129.6 (C-3'), 121.0 (C-4'), 114.6 (C-2'), 117.6 (C-3), 68.8 (C-1).

**Theoretical Methods.** The stationary points on the potential energy surface for the model reaction of KF with ethyl bromide catalyzed by 18-crown-6 and the diols BDMb and PDIOL were obtained by geometry optimization using the PBE functional.<sup>30</sup> For these optimizations, the def2-SVP basis set<sup>31</sup> was used for carbon, hydrogen, and potassium, and the ma-def2-SVP basis set<sup>32</sup> was used for oxygen, fluorine, and bromine. Harmonic frequency calculations were done for the optimized structures to obtain the vibrational, rotational, and translations contributions to the free energy. Aimed to obtain more accurate electronic energies, single point energy calculations were done at M06-2X,<sup>33</sup> MP2, and LPNO-CEPA/1<sup>34–37</sup> levels of theory. The M06-2X and MP2 calculations were done with the def2-TZVPP basis set<sup>31</sup> for carbon, hydrogen, and potassium, and the ma-def2-TZVPP basis set<sup>32</sup> for oxygen, fluorine, and bromine. The LPNO-CEPA/1 calculations were done with the smaller ma-def2-SVP basis set (as defined above), and the estimation of the LPNO-CEPA energies with the higher ma-def2-TZVPP basis set was done by the additivity approximation of the correlation energy:<sup>38,39</sup>

$$E(\text{CEPA/ma} - \text{def2} - \text{TZVPP}) \\ \cong E(\text{CEPA/ma} - \text{def2} - \text{SVP}) + E(\text{MP2/ma} - \text{def2} \\ - \text{TZVPP}) - E(\text{MP2/ma} - \text{def2} - \text{SVP}) \quad (6)$$

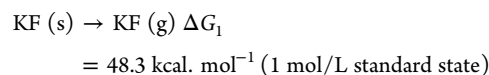
The MP2 calculations were done with the resolution of identity approximation, and all the electrons were correlated in the CEPA and MP2 calculations. The LPNO-CEPA energies were considered the best level of theory, and the respective energies were used for obtaining the free energy profile.

The solvent effect was included through single-point energy calculations using the SMD method.<sup>40</sup> The X3LYP functional<sup>41</sup> with the 6-31(+)-G(d) basis set was used for the electronic density in the SMD computations. Thus, the present calculations of the free energy are a composite method and the free energy for each species in the solution phase (acetonitrile solvent) is given by:

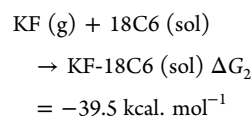
$$G_{\text{sol}} = E_{\text{el}} + G_{\text{vrt}} + \Delta G_{\text{solv}} + 1.89 \text{ kcal mol}^{-1} \quad (7)$$

where  $E_{\text{el}}$  is the electronic energy calculated by the LPNO-CEPA method,  $G_{\text{vrt}}$  is the vibrational, rotational, and translational contribution to the free energy (1 atm),  $\Delta G_{\text{solv}}$  is the solvation free energy, and the 1.89 kcal mol<sup>-1</sup> is the correction from 1 atm to the 1 mol L<sup>-1</sup> standard state. Thus, the final solution phase free energy,  $G_{\text{sol}}$  corresponds to the 1 mol L<sup>-1</sup> standard state. In some structures, there are additional imaginary modes due to almost free rotation of methyl groups and the formation of supramolecular complexes. We have corrected the vibrational partition function to make equal number of degrees of freedom for each side in the reaction equation.

Because the KF salt is a solid, experimental thermodynamics data must be included for correct description of its solubilization. In our approach, we have considered the free energy for sublimation of the KF salt taken from NIST:



and calculated the process:



where (s) means solid, (g) means gas, and (sol) means solution phase. Thus, combining the two equations, we have the solubilization free energy of KF by the 18C6:



All the PBE, M06-2X, MP2, and LPNO-CEPA calculations were done with the ORCA 3 program,<sup>42,43</sup> whereas the SMD calculations were done with the GAMESS program.<sup>44,45</sup>

In the calculations of  $\Delta G^\ddagger$  in the liquid phase, we have used the separable equilibrium solvation approach,<sup>46</sup> which is based on the rigorous formulation of the transition state theory. Empirical translational entropy correction, which does not have any theoretical support, was not included.

## ■ ASSOCIATED CONTENT

### Supporting Information

The Supporting Information is available free of charge at <https://pubs.acs.org/doi/10.1021/acs.joc.0c02229>.

Coordinates of the optimized structures and table of the calculations (PDF)

## AUTHOR INFORMATION

## Corresponding Author

Josefredo R. Pliego, Jr – Departamento de Ciências Naturais, Universidade Federal de São João del-Rei, São João del-Rei 36301-160, MG, Brazil; [orcid.org/0000-0002-2944-5332](https://orcid.org/0000-0002-2944-5332); Email: [pliego@ufsj.edu.br](mailto:pliego@ufsj.edu.br)

## Authors

Samuel L. Silva – Departamento de Ciências Naturais, Universidade Federal de São João del-Rei, São João del-Rei 36301-160, MG, Brazil

Marcelo S. Valle – Departamento de Ciências Naturais, Universidade Federal de São João del-Rei, São João del-Rei 36301-160, MG, Brazil

Complete contact information is available at:  
<https://pubs.acs.org/10.1021/acs.joc.0c02229>

## Notes

The authors declare the following competing financial interest(s): A patent application was filled.

## ACKNOWLEDGMENTS

The authors thank the agencies CNPq, FAPEMIG, and CAPES for support.

## REFERENCES

- (1) Lee, J.-W.; Oliveira, M. T.; Jang, H. B.; Lee, S.; Chi, D. Y.; Kim, D. W.; Song, C. E. Hydrogen-bond promoted nucleophilic fluorination: Concept, mechanism and applications in positron emission tomography. *Chem. Soc. Rev.* **2016**, *45*, 4638–4650.
- (2) Liang, S.; Hammond, G. B.; Xu, B. Hydrogen bonding: Regulator for nucleophilic fluorination. *Chem. – Eur. J.* **2017**, *23*, 17850–17861.
- (3) Kim, D. W.; Jeong, Lim, S. T.; Sohn, M.-H.; Katzenellenbogen, J. A.; Chi, D. Y. Facile nucleophilic fluorination reactions using tert-alcohols as a reaction medium: Significantly enhanced reactivity of alkali metal fluorides and improved selectivity. *J. Org. Chem.* **2008**, *73*, 957–962.
- (4) Kim, D. W.; Ahn, D. S.; Oh, Y. H.; Lee, S.; Kil, H. S.; Oh, S. J.; Lee, S. J.; Kim, J. S.; Ryu, J. S.; Moon, D. H.; et al. A new class of  $sn_2$  reactions catalyzed by protic solvents: Facile fluorination for isotopic labeling of diagnostic molecules. *J. Am. Chem. Soc.* **2006**, *128*, 16394–16397.
- (5) Oh, Y. H.; Ahn, D. S.; Chung, S. Y.; Jeon, J. H.; Park, S. W.; Oh, S. J.; Kim, D. W.; Kil, H. S.; Chi, D. Y.; Lee, S. Facile  $sn_2$  reaction in protic solvent: Quantum chemical analysis. *J. Phys. Chem. A* **2007**, *111*, 10152–10161.
- (6) Parker, A. J. Protic-dipolar aprotic solvent effects on rates of bimolecular reactions. *Chem. Rev.* **1969**, *69*, 1.
- (7) Pliego, J. R., Jr. Molecular dynamics and cluster-continuum insights on bulk alcohols effects on  $S_N2$  reactions of potassium and cesium fluorides with alkyl halides. *J. Mol. Liq.* **2017**, *237*, 157–163.
- (8) Liotta, C. L.; Harris, H. P. Chemistry of naked anions. I. Reactions of the 18-crown-6 complex of potassium fluoride with organic substrates in aprotic organic solvents. *J. Am. Chem. Soc.* **1974**, *96*, 2250–2252.
- (9) Pliego, J. R., Jr.; Riveros, J. M. New insights on reaction pathway selectivity promoted by crown ether phase-transfer catalysis: Model ab initio calculations of nucleophilic fluorination. *J. Mol. Catal. A - Chem.* **2012**, *363-364*, 489–494.
- (10) Pliego, J. R. Potassium fluoride activation for the nucleophilic fluorination reaction using 18-crown-6, [2.2.2]-cryptand, pentaethylene glycol and comparison with the new hydro-crown scaffold: A theoretical analysis. *Org. Biomol. Chem.* **2018**, *16*, 3127–3137.
- (11) Jadhav, V. H.; Jang, S. H.; Jeong, H.-J.; Lim, S. T.; Sohn, M.-H.; Kim, J.-Y.; Lee, S.; Lee, J. W.; Song, C. E.; Kim, D. W. Oligoethylene glycols as highly efficient multifunctional promoters for nucleophilic substitution reactions. *Chem. – Eur. J.* **2012**, *18*, 3918–3924.
- (12) Lee, J. W.; Yan, H.; Jang, H. B.; Kim, H. K.; Park, S.-W.; Lee, S.; Chi, D. Y.; Song, C. E. Bis-terminal hydroxy polyethers as all-purpose, multifunctional organic promoters: A mechanistic investigation and applications. *Angew. Chem., Int. Ed.* **2009**, *48*, 7683–7686.
- (13) Han, H. J.; Lee, S.-S.; Kang, S. M.; Kim, Y.; Park, C.; Yoo, S.; Kim, C. H.; Oh, Y.-H.; Lee, S.; Kim, D. W. The effects of structural modifications of bis-tert-alcohol-functionalized crown-calix[4]arenes as nucleophilic fluorination promoters and relations with computational predictions. *Eur. J. Org. Chem.* **2020**, *2020*, 728–735.
- (14) Kang, S. M.; Kim, C. H.; Lee, K. C.; Kim, D. W. Bis-triethylene glycolic crown-5-calix[4]arene: A promoter of nucleophilic fluorination using potassium fluoride. *Org. Lett.* **2019**, *21*, 3062–3066.
- (15) Jadhav, V. H.; Choi, W.; Lee, S.-S.; Lee, S.; Kim, D. W. Bis-tert-alcohol-functionalized crown-6-calix[4]arene: An organic promoter for nucleophilic fluorination. *Chem. – Eur. J.* **2016**, *22*, 4515–4520.
- (16) Carvalho, N. F.; Pliego, J. R., Jr. Theoretical design and calculation of a crown ether phase-transfer-catalyst scaffold for nucleophilic fluorination merging two catalytic concepts. *J. Org. Chem.* **2016**, *81*, 8455–8463.
- (17) Dalessandro, E. V.; Pliego, J. R. Theoretical design of new macrocycles for nucleophilic fluorination with KF: Thiourea-crown-ether is predicted to overcome the [2.2.2]-cryptand. *Mol. Syst. Des. Eng.* **2020**, 1513.
- (18) Pliego, J. R. First solvation shell effects on ionic chemical reactions: New insights for supramolecular catalysis. *J. Phys. Chem. B* **2009**, *113*, 505–510.
- (19) Pliego, J. R.; Piló-Veloso, D. Chemoselective nucleophilic fluorination induced by selective solvation of the  $sn_2$  transition state. *J. Phys. Chem. B* **2007**, *111*, 1752–1758.
- (20) Pliego, J. R. Mechanism of nucleophilic fluorination promoted by bis-tert-alcohol-functionalized crown-6-calix[4]arene. *Int. J. Quantum Chem.* **2018**, *118*, No. e25648.
- (21) Silva, S. L.; Valle, M. S.; Pliego, J. R., Jr. Micro-solvation and counter ion effects on ionic reactions: Activation of potassium fluoride with 18-crown-6 and tert-butanol in aprotic solvents. *J. Mol. Liq.* **2020**, *319*, 114211.
- (22) Landini, D.; Maia, A.; Rampoldi, A. Dramatic effect of the specific solvation on the reactivity of quaternary ammonium fluorides and poly(hydrogen fluorides),  $(HF)_n \cdot n \cdot F^-$ , in media of low polarity. *J. Org. Chem.* **1989**, *54*, 328–332.
- (23) Albanese, D.; Landini, D.; Penso, M. Hydrated tetrabutylammonium fluoride as a powerful nucleophilic fluorinating agent. *J. Org. Chem.* **1998**, *63*, 9587–9589.
- (24) Pliego, J. R., Jr. Chemical reactions inside structured nano-environment:  $S_N2$  vs.  $E_2$  reactions for the  $F^- + CH_3CH_2Cl$  system. *Phys. Chem. Chem. Phys.* **2011**, *13*, 779–782.
- (25) Kim, D. W.; Jeong, H.-J.; Lim, S. T.; Sohn, M.-H. Facile nucleophilic fluorination of primary alkyl halides using tetrabutylammonium fluoride in a tert-alcohol medium. *Tetrahedron Lett.* **2010**, *51*, 432–434.
- (26) Engle, K. M.; Pfeifer, L.; Pidgeon, G. W.; Giuffredi, G. T.; Thompson, A. L.; Paton, R. S.; Brown, J. M.; Gouverneur, V. Coordination diversity in hydrogen-bonded homoleptic fluoride-alcohol complexes modulates reactivity. *Chem. Sci.* **2015**, *6*, 5293–5302.
- (27) Pfeifer, L.; Engle, K. M.; Pidgeon, G. W.; Sparkes, H. A.; Thompson, A. L.; Brown, J. M.; Gouverneur, V. Hydrogen-bonded homoleptic fluoride–diaryliurea complexes: Structure, reactivity, and coordinating power. *J. Am. Chem. Soc.* **2016**, *138*, 13314–13325.
- (28) Iwasaki, T.; Fukuoka, A.; Yokoyama, W.; Min, X.; Hisaki, I.; Yang, T.; Ehara, M.; Kuniyasu, H.; Kambe, N. Nickel-catalyzed coupling reaction of alkyl halides with aryl grignard reagents in the presence of 1,3-butadiene: Mechanistic studies of four-component coupling and competing cross-coupling reactions. *Chem. Sci.* **2018**, *9*, 2195–2211.

- (29) Joo, S.-R.; Lim, I.-K.; Kim, S.-H. An alternative route for boron phenoxide preparation from arylboronic acid and its application for CO bond formation. *Tetrahedron Lett.* **2020**, *61*, 152197.
- (30) Perdew, J. P.; Burke, K.; Ernzerhof, M. Generalized gradient approximation made simple. *Phys. Rev. Lett.* **1996**, *77*, 3865–3868.
- (31) Weigend, F.; Ahlrichs, R. Balanced basis sets of split valence, triple zeta valence and quadruple zeta valence quality for h to rn: Design and assessment of accuracy. *Phys. Chem. Chem. Phys.* **2005**, *7*, 3297–3305.
- (32) Zheng, J.; Xu, X.; Truhlar, D. G. Minimally augmented karlsruhe basis sets. *Theor. Chem. Acc.* **2011**, *128*, 295–305.
- (33) Zhao, Y.; Truhlar, D. G. The M06 suite of density functionals for main group thermochemistry, thermochemical kinetics, non-covalent interactions, excited states, and transition elements: Two new functionals and systematic testing of four M06-class functionals and 12 other functionals. *Theor. Chem. Acc.* **2008**, *120*, 215–241.
- (34) Kollmar, C.; Neese, F. The coupled electron pair approximation: Variational formulation and spin adaptation. *Mol. Phys.* **2010**, *108*, 2449–2458.
- (35) Neese, F.; Wennmohs, F.; Hansen, A. Efficient and accurate local approximations to coupled-electron pair approaches: An attempt to revive the pair natural orbital method. *J. Chem. Phys.* **2009**, *130*, 114108.
- (36) Neese, F.; Hansen, A.; Wennmohs, F.; Grimme, S. Accurate theoretical chemistry with coupled pair models. *Acc. Chem. Res.* **2009**, *42*, 641–648.
- (37) Wennmohs, F.; Neese, F. A comparative study of single reference correlation methods of the coupled-pair type. *Chem. Phys.* **2008**, *343*, 217–230.
- (38) Curtiss, L. A.; Raghavachari, K.; Trucks, G. W.; Pople, J. A. Gaussian-2 theory for molecular energies of first- and second-row compounds. *J. Chem. Phys.* **1991**, *94*, 7221.
- (39) Nobes, R. H.; Bouma, W. J.; Radom, L. The additivity of polarization function and electron correlation effects in ab initio molecular-orbital calculations. *Chem. Phys. Lett.* **1982**, *89*, 497.
- (40) Marenich, A. V.; Cramer, C. J.; Truhlar, D. G. Universal solvation model based on solute electron density and on a continuum model of the solvent defined by the bulk dielectric constant and atomic surface tensions. *J. Phys. Chem. B* **2009**, *113*, 6378–6396.
- (41) Xu, X.; Zhang, Q.; Muller, R. P.; Goddard, W. A., III An extended hybrid density functional (x3lyp) with improved descriptions of nonbond interactions and thermodynamic properties of molecular systems. *J. Chem. Phys.* **2005**, *122*, 014105–014114.
- (42) Neese, F.; Wennmohs, F.; Becker, U.; Riplinger, C. The orca quantum chemistry program package. *J. Chem. Phys.* **2020**, *152*, 224108.
- (43) Neese, F. The ORCA program system. *WIREs Comput. Mol. Sci.* **2012**, *2*, 73–78.
- (44) Barca, G. M. J.; Bertoni, C.; Carrington, L.; Datta, D.; de Silva, N.; Deustua, J. E.; Fedorov, D. G.; Gour, J. R.; Gunina, A. O.; Guidez, E.; et al. Recent developments in the general atomic and molecular electronic structure system. *J. Chem. Phys.* **2020**, *152*, 154102.
- (45) Schmidt, M. W.; Baldrige, K. K.; Boatz, J. A.; Elbert, S. T.; Gordon, M. S.; Jensen, J. H.; Koseki, S.; Matsunaga, N.; Nguyen, K. A.; Su, S.; et al. General atomic and molecular electronic structure system. *J. Comput. Chem.* **1993**, *14*, 1347–1363.
- (46) Chuang, Y. Y.; Cramer, C. J.; Truhlar, D. G. The interface of electronic structure and dynamics for reactions in solution. *Int. J. Quant. Chem.* **1998**, *70*, 887–896.